Eur Biophys J (1998) 28: 1–11 © Springer-Verlag 1998

ARTICLE

Horst Ruf · Barry J. Gould

Size distributions of chylomicrons from human lymph from dynamic light scattering measurements

Received: 12 October 1997 / Revised version: 26 June 1998 / Accepted: 7 August 1998

Abstract Chylomicrons, the vehicles for the transport of exogeneous triglycerides and cholesterol in the lymph and the blood, were characterized by their size from dynamic light scattering measurements. To achieve an appropriate resolution, correlation data were collected over several hours. Analysis was performed with an extended version of the regularization method CONTIN, and special attention was given to errors in the experimental baseline and to randomness of the residuals. The solutions selected by means of Fisher's F-test by CONTIN agreed with those obtained with the stability plot of Schnablegger and Glatter, when in the case of data of lower statistical accuracy the solution was taken from the lower part of the confidence interval of the F-test. The intensity-weighted size distributions indicated two classes of particle, their mean diameters being 100–140 nm and 330–350 nm. The ability to resolve two peaks of such a size ratio is demonstrated. The numbers of particles associated with the two peaks were estimated by means of the scattering properties of the particles, which showed that the overwhelming majority were small ones. This estimation also suggested that the mean size of the first peak of the number distribution is significantly smaller than the typical size of chylomicrons. This was consistent with the finding that the sample contained not only apolipoprotein B-48 but also a similar amount of apolipoprotein B-100, which is associated with lipoproteins of smaller size. The larger particles of the second peak are probably dietary triglyceride-rich chylomicrons.

Key words Chylomicrons · Dynamic light scattering · Size distribution · F-test · Stability plot

H. Ruf (✉)
Max-Planck-Institut für Biophysik,
Kennedyallee 70,
D-60596 Frankfurt a. M., Germany
e-mail: ruf@biophys.mpg.de

B. J. Gould
School of Biological Sciences,
University of Surrey,
Guildford, Surrey GU2 5XH, UK

Introduction

Chylomicrons are lipoprotein particles which are used to transport dietary lipid. They are synthesized in enterocytes, secreted, and enter the circulation via the thoracic lymph duct. Chylomicrons are large particles which are converted to smaller chylomicron remnants, by the action of lipoprotein lipase, before being taken up by hepatocytes. There are other lipoprotein particles in the circulation which are classified by their density into very low density (VLDL), intermediate density (IDL), low density (LDL), and high density (HDL) lipoprotein particles. The density increases as the percentage protein content increases and the lipid content and particle size decreases.

Dynamic light scattering (DLS) is a frequently applied method in size characterization of colloidal particles, and has also been used to determine sizes of lipoproteins (Vuaridel-Bonanomi and Weder 1991; Nenseter et al. 1992). The advantages of this non-invasive, direct method are that one measures the particles in liquid suspension without the need for further calibration. DLS is a rapid method when the mean size of a particle population is to be determined, but requires much longer measurements when greater detail needs to be resolved (Pike et al. 1983), as shown for binary mixtures of calibrated polystyrene latex particles (Flamberg and Pecora 1984; Morrison et al. 1985; Ruf et al. 1993) and lipid vesicles (Stelzer et al. 1983; Hallett et al. 1991; Ruf et al. 1992; Egelhaaf et al. 1996). Despite these successful applications of DLS, deriving the size distribution of macromolecules with great accuracy is often considered to be a difficult problem. This has to do with the different sampling schemes applied for the measurements, the differences in the results obtained with different evaluation methods, the statistical accuracy of the data that is assumed to be sufficient, and the ability to eliminate systematic errors such as those caused by an error in the experimental baseline. In this paper we concentrate on the latter two points.

The size distributions were determined with the algorithm CONTIN (Provencher et al. 1978; Provencher 1979,

1982 a, b), which is one of the evaluation techniques devised to cope with the ill-posed nature of data inversion, that is, with the fact that large differences in size distributions are often only weakly expressed in the corresponding autocorrelation functions, through which even small experimental errors can have a very strong influence on the results. This method employs a regularizor (Phillips 1962) to impose smoothness or simplicity on the size distribution. The optimal solution, which is considered to represent the best compromise between the opposing demands of minimum sum of squared residuals (variance) and simplicity of the size distribution, is determined by means of Fisher's F-test, which compares the variance of each of the differently regularized solutions with that of the least square solution, which is taken as a reference. For comparison, we also used the stability plot introduced by Schnablegger and Glatter (1991), which utilizes properties of the regularizor itself for the selection of an appropriately regularized solution.

The purpose of this work is to show that mixtures of lipoprotein particles can be characterized with appropriate resolution by means of DLS. For these investigations we have studied human lymph, which contains mainly newly synthesized chylomicrons, as an example of a lipoprotein sample.

Materials and methods

Chylomicrons

Human lymph

Human thoracic duct lymph samples from a patient undergoing thoracic surgery were kindly supplied by Dr. J. Wright (Royal Surrey County Hospital, Guildford, UK). This was treated with preservative 5% (v/v) according to the method of Edelstein and Scanu (1986), to prevent degradation, and was stored frozen at −20 °C. The preservative contained EDTA, sodium azide, sodium chloride (Merck, Lutterworth, UK), aprotinin, benzamidine, chloramphenicol, and gentamicin sulfate (Sigma, Poole, UK). The lymph contained apolipoprotein (apo) B-48 and apo B-100 containing particles.

Chylomicron enriched samples

The lymph samples were overlayered with equal volumes of saline solution (1.006 g/ml), and ultracentrifuged for 5.0×10^6 g_{max} min (Lindgren et al. 1972) to prepare the chylomicron enriched samples using essentially the method of Grundy and Mok (1965). This allowed the flotation and concentration of larger, less-dense triglyceride-rich lipoprotein particles of densities < 1.006 g/ml, which were mainly chylomicrons. In the case of the sample utilized for density gradient centrifugation, the apo B-100 and apo B-48 content of these particles was determined by analytical sodium dodecyl sulfate polyacrylamide gel electrophoresis followed by staining with Coomassie blue and densitometry by the method of Karpe and Hamsten (1994). The concentrations of apo B-48 and apo B-100 were 19.1 and 42.9 μg/ml, respectively. This electrophoresis also showed that the apolipoproteins were not degraded.

Density gradient centrifugation

Chylomicrons were separated into fractions, with a narrow particle size, in a continuous sucrose density gradient using the method similar to that of Zilversmit (1969). Stock solutions of 30%, 50%, and 60% sucrose (w/v) were prepared in 0.9% (w/v) saline solution. The densities of the sucrose solutions were confirmed by refractometry. The density of 1 ml of the chylomicron enriched sample was increased by mixing it with 5 ml of the 60% sucrose solution. Five ml of 60% sucrose solution were placed in a 30 ml centrifuge tube; this was carefully overlayered with 0.8 ml of the density adjusted chylomicron sample. A linear sucrose gradient, from 50% to 30% sucrose, was then slowly pumped into the tube. These tubes were centrifuged in a Beckman L7 ultracentrifuge with a Beckman SW 25.1 swing-out rotor (Beckman Instruments, High Wycombe, UK) at 15 000 rpm for 1 h at 20 °C to give a total force of 1.8×10^6 g min. After completion of centrifugation the gradient was immediately unloaded by upward displacement using the 60% sucrose solution and separated into 5 ml fractions (DG1, DG2, DG3, DG4, and DG5) which were then stored at 4 °C. The gradient former and unloading devices were supplied by MSE Scientific Equipment, Crawley, UK.

Dynamic light scattering

Theoretical

The theory of the DLS method can be found in many textbooks and reviews. We present here the equations necessary for this analysis. The fluctuations of the scattered intensity measured at a given angle are analyzed by calculating the photocount autocorrelation function $C(\tau_k)$ for a set of delay times τ_k. This function is related to the "measured" normalized electric field autocorrelation function, $g^{(1)}_{exp}(\tau_k)$, by the Siegert relation (Siegert 1943):

$$C(\tau_k)=B(1+\beta\,|\,g^{(1)}_{exp}(\tau_k)\,|^2) \tag{1}$$

where B is a measured baseline, and β is an instrumental coherence factor. In our case, B is determined from the mean photon count per sampling time interval.

The electric field autocorrelation function, $g^{(1)}(\tau_k)$, of a polydisperse sample of particles expressed in terms of the linewidth distribution $s(\Gamma)$ is given by

$$\left|\, g^{(1)}(\tau_k)\,\right| = \int_0^\infty s(\Gamma)\exp(-\Gamma\,\tau_k)\,\mathrm{d}\Gamma \tag{2}$$

The characteristic line width, $\Gamma = q^2 D$, is proportional to the diffusion constant D of particles of a given size, and to the square of the magnitude of the scattering vector $q = (4\pi n_s/\lambda) \sin(\Theta/2)$, where n_s is the index of refraction of the solvent, λ the wavelength in vacuo of the incident light, and Θ the scattering angle. $s(\Gamma)\,d\Gamma$ represents the fraction of light scattered by particles with linewidths between Γ and $\Gamma + d\Gamma$ in the direction of Θ.

For spherical particles, using the Stokes-Einstein equation

$$D = kT/6\pi\eta R \tag{3}$$

where R is the hydrodynamic radius, k Boltzmann's constant, T the absolute temperature, η the viscosity of the solvent, and the relationship (Flamberg and Pecora 1984)

$$I(R) = s(\Gamma)\,(d\Gamma/dR) \tag{4}$$

the electric field autocorrelation function $g^{(1)}(\tau_k)$ can be expressed in terms of the intensity-weighted size distribution $I(R)$. With $b = q^2\,kT/6\pi\eta$, Eq. (2) reads

$$\left| g^{(1)}(\tau_k) \right| = \int_0^\infty I(R) \exp(-(b/R)\,\tau_k)\,dR \tag{5}$$

Either $s(\Gamma)$ or $I(R)$ can be obtained from CONTIN analysis. We generally determine $I(R)$ and calculate the mean size from the moments

$$M_j = \int_0^\infty R^j\, I(R)\,dR \tag{6}$$

according to the commonly used definition M_1/M_0. The average size M_0/M_{-1} defined by Flamberg and Pecora (1984) is determined when making a comparison with results from the cumulant method (Koppel 1972) or with the mean size derived by means of Eq. (3) from the mean linewidth resulting from CONTIN analysis with the $s(\Gamma)$ option.

Experimental

Sample preparation. Both chylomicron samples were prepared in unbuffered solution with neutral pH. The first sample, denoted as DG0, was prepared from a sample containing 50% (w/w) sucrose by diluting 200 µl of this sample with 570 µl distilled water to yield a final sucrose concentration of 13% (w/w), and was filtered through a 0.8 µm Nuclepore polycarbonate filter directly into a cylindrical cuvette (inner diameter 8 mm; Hellma, Müllheim, Germany). For the second sample, chylomicron II, 100 µl of a chylomicron enriched sample were diluted with 1 ml of saline solution (1.006 g/ml), and centrifuged for 15 min at 12 000 rpm (Zentrifuge 5412, Eppendorf, Hamburg, Germany) to float up large particles, which were not observed in the first case and which were likely due to a longer storage. The larger particles were removed thoroughly with a pipette, and the remaining solution was filtered as before through a 0.8 µm Nuclepore polycarbonate filter.

Table 1 Experimental conditions of dynamic light scattering measurements. *B* is the baseline of the photocount autocorrelation function obtained by summing up the raw data of the corresponding individual measurements, and is a measure of data accuracy. The values given in this table were rounded to the first digit. The coherence factor β was obtained from cumulant analysis; it is equal to the intercept of the corresponding normalized photocount autocorrelation function minus one

Sample	Mean count rate (kcps)	No. of data channels	Sampling time (µs)	No. of samples	*B*	β
Chylo I (DG0)	~30	136	30	2.2×10^8	1.8×10^8	0.64
Chylo II	~80	256	10	5.36×10^9	3.2×10^9	0.97

Experimental set-up and measurements. The light scattering apparatus (ALV Langen, Germany) was of standard design and has been described elsewhere (Georgalis et al. 1987). Distilled water, the temperature of which was kept constant at 20 °C, was used as the index matching fluid surrounding the sample cell, and the scattering angle was 90 °C. The measurements were performed with slightly different set-ups. The chylomicron sample DG0 was measured using a Spectra Physics, Model 124 B, 15 mW, linearly polarized HeNe laser, and the signals from the detection unit (Malvern Model RF 313) were collected with a Brookhaven BI 2020, 144 channels, 4-bit correlator (Brookhaven Instruments, Holtsville, N.Y., USA). The other sample, chylomicron II, was measured with a modified set-up. The light source was a NEC, Model GLG 5740, 50 mW, linearly polarized HeNe laser (GFO, Hamburg, Germany), and the scattered light was detected through fiber optics (single mode fiber 633-FC with pigtail collimator, Spindler & Hoyer, Göttingen, Germany) with a coherence factor $\beta \approx 1$ (Gisler et al. 1995). The signals from a detection unit (Model 9863, Brookhaven Instruments) were collected with a Brookhaven BI 9000AT multi-bit correlator. The experimental conditions used for the measurements carried out with equidistant spacing of the delay time channels are summarized in Table 1. Measurements were carried out in the batch mode, where individual measurements were done for 5 min with the first set-up, as described previously (Ruf et al. 1992), and for 1 min with the second set-up. Each individual measurement was normalized with respect to its baseline prior to averaging to give the final data for analysis, as this method reduces the effects of drift in the laser intensity. The value of baseline *B*, which is used as a measure of data accuracy, was obtained by summing up the (unnormalized) raw data of the measurements of each batch. The range of delay times used for measuring the photocount autocorrelation function was chosen to span roughly two mean characteristic decay times. The mean intensity of the scattered light was restricted to count rates smaller than about 80 kcps, which keeps the noise in the data nearly random. We have found that the F-test returns too weakly regularized solutions when data contain errors due to an inaccurate value of the experimental baseline (normalization errors), and fre-

quently when measuring at higher scattering intensity where nonrandom intensity fluctuation noise (Saleh and Cardoso 1973) becomes dominant.

Data analysis

Size distributions were determined using only data with baseline values larger than 10^8 with an extended version (Ruf 1989; Ruf et al. 1992) of the constrained regularization method CONTIN. The regularizor was the overall curvature of the size distribution (Phillips 1962). The data used for all analyses were restricted to values of the normalized photocount autocorrelation function > 1.01. Other specifications were to impose no zero constraints on the amplitudes of the intensity distribution at the two integration limits by setting the control parameters NENDZ equal to zero, and the solutions selected here were taken from the final weighted analysis and from the confidence interval of the F-test (Provencher 1979, 1982 a). Numerical integration of Eq. (5) was carried out using Simpson's rule with $N_g = 69$ or 70 grid points. The data points of the first two delay times were omitted to reduce possible effects due to afterpulsing. Hence, data sets with 134 or 254 points were analyzed depending on the correlator in use. The relative error in the experimental baseline of the normalized photocount autocorrelation function, $\Delta B/B$, was determined in two steps. A first estimate was obtained by fitting the normalization error function (NEF) as described elsewhere (Ruf 1989; Ruf et al. 1992). This value was then refined by means of procedure which avoids the problems of overfitting the data when fitting additional parameters. This procedure, which is similar to the method for adjusting the baseline with the regularization method ORT (Schnablegger and Glatter 1991), will be described in a forthcoming paper. For final analysis the data was corrected for the error in the baseline as described in Ruf (1989).

The program CONTIN carries out a series of fits with different degrees of regularization, where instead of the variance alone a combination of variance and regularizor, called the objective function F_{ob}, is minimized (Provencher 1982 a), and determines an appropriately regularized solution by means of the F-test. This test defines a confidence interval which is associated with a set of solutions rather than a single one. Provencher (1979) suggested that the solution with a PROB1(α) value nearest to 0.5 should be accepted, but he also pointed out that other solutions might be considered (Provencher 1982 a, 1992). The relative change in variance with regard to that of the reference solution ($\alpha_0 \approx 0$) or fractional increase

$$V_f(\alpha / s_1) = \frac{V(\alpha / s_1) - V(\alpha_0 / s_1)}{V(\alpha_0 / s_1)} \tag{7}$$

is one of the elements of the F-test, and this is plotted against the regularization parameter to show the changes in the sum of squared residuals of the various solutions. We used α/s_1 instead of α for the x-axis since this quantity has a fixed starting point (Provencher 1982 b).

The plot of the logarithm of the magnitude of the regularizor, denoted as the norm of the solution, against the logarithm of the regularization parameter is called the stability plot (Schnablegger and Glatter 1991). The correct Langrange multiplier or regularization parameter is found by taking the point of inflection of a region, where the solution is nearly independent from the regularization parameter, and where the fractional increase in variance is still small. We have adapted this method to our CONTIN analysis to compare its results with those of the F-test. The quantity

$$N_s(\alpha / s_1) = \left[\frac{F_{ob}(\alpha / s_1) - V(\alpha / s_1)}{(\alpha / s_1)^2} \right]^{1/2} \tag{8}$$

is proportional to the solution norm. All quantities needed for the calculation of V_f and N_s were taken from the output of CONTIN.

The data from the fractionated samples and the data of the individual measurements of the batches were analysed using a third-order cumulant analysis. In the latter cases this method was used to check for sample stability and for the occurrence of outliers due to dust. The lack of outliers indicated that the suspension was quite clean and, moreover, that the chylomicron samples were remarkably stable over days (Ruf and Gould 1997). The fractionated samples obtained after sucrose density gradient centrifugation were too dilute for the collection of data of sufficient statistical accuracy within reasonable measuring times. Therefore, for these samples only mean diameters were determined. The more reliable data from our first chylomicron sample DG0 ($B = 1.8\times10^8$) was analyzed with both the $s(\Gamma)$ option of CONTIN and the cumulant method. All analyses were performed with the same data points. To obtain a good fit four cumulants were needed, while in the case of the individual 5 min measurements which had baselines of the order of 10^7, three cumulants were generally sufficient, in agreement with the limitations discussed by Chu et al. (1985). There are strong, clear criteria for a decision in favor of a four-cumulants fit instead of a three-cumulants fit: a significant reduction of variance, a significant reduction of systematic deviations in the residual pattern, and convergence to the mean diameter obtained from CONTIN analysis with the $s(\Gamma)$ option.

Simulated data

Computer-generated data simulating the autocorrelation function of a bimodal size distribution of a peak size ratio of 1 : 2.6 were obtained with a method similar to that of Nyeo and Chu (1989). We used Gaussians instead of lognormal functions as we were determining size distributions in terms of particle sizes instead of characteristic linewidths. The two Gaussians had the same mean diameters and covered the same fractions as the two peaks of the distribution determined from the chylomicron sample DG0. Standard deviations of the Gaussians were 40 nm and 66 nm. Different levels of noise were added using baseline values B of 1×10^7, 2×10^8, and 3×10^9 (coherence factor $\beta = 0.64$, number of data points 136, sampling time 30 μs).

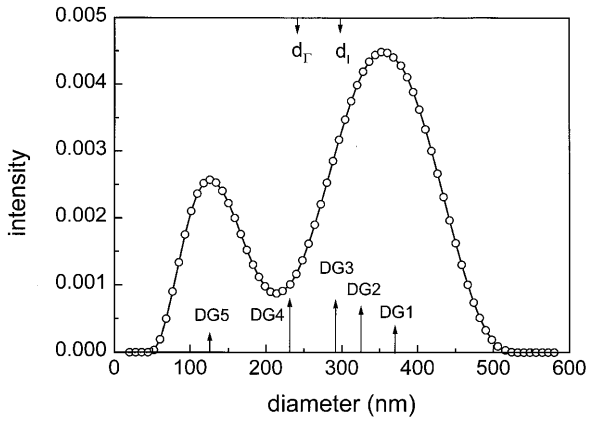

Fig. 1 Chylomicron sample DG0. Intensity-weighted size distribution normalized to 1 as determined by CONTIN with PROB1 (α) = 0.5 from data corrected for normalization errors ($\Delta B/B = -7\times10^{-3}$) using a size range of 20–580 nm. The intensity-weighted mean diameter from the analysis with the $I(R)$ option is denoted by d_I and the corresponding mean diameter from analysis with the $s(\Gamma)$ option, from the definition of Flamberg and Pecora (1984) and from cumulant analysis by d_Γ. The differences of the two mean values is due to different weightings by $s(\Gamma)$ and $I(d)$. DG1 to DG5 indicate the mean diameters obtained from cumulant analysis for the fractions after separation by sucrose density gradient centrifugation. The heights of the arrows are proportional to the mean intensity scattered by these samples at the same intensity of incident light, which was determined from the total number of photons counted during the experiments. Since only their relative heights are of interest, the values of intensity or count rate are not specified. Taking into account that the corresponding intensity weighted mean values of the sizes would be shifted towards larger values, the intensity profile of the separated samples agrees well with the intensity distribution of the chylomicron sample DG0

Table 2 Mean diameters of chylomicrons d_Γ obtained from the cumulant analysis. DG0 represents the original sample of chylomicrons. DG1 to DG5 are the various fractions obtained from density gradient centrifugation. Refractive indices, n_s, and viscosity, η, at 20 °C of the corresponding sucrose-water mixtures were taken from Lide (1975–1976) and linearly interpolated if necessary. v is the average count rate of the dynamic light scattering experiment, $\delta\tau$ the sampling time, and N_{tot} the total number of samples from which the corresponding autocorrelation functions are calculated. The sample DG0, originally in 50% sucrose in water, was diluted with distilled water to allow the use of shorter sampling times for the DLS experiments

Sample	% sucrose in water (w/w)	n_s	η (cp)	v (s^{-1})	$\delta\tau$ (μs)	N_{tot}	d_Γ (nm)
DG0	13.0	1.352	1.48	30000	30	2.2×10^8	239
DG1	31.7	1.384	3.66	803	120	2.2×10^7	371
DG2	35.0	1.390	4.33	1110	120	2.0×10^7	324
DG3	38.3	1.397	5.44	1420	150	2.0×10^7	292
DG4	41.7	1.400	7.04	1400	150	1.5×10^7	232
DG5	45.0	1.410	9.43	523	120	1.5×10^7	125

Results

The size distribution of the scattered intensity of the original chylomicron enriched sample DG0 obtained using CONTIN analysis is depicted in Fig. 1 (instead of the hydrodynamic radius the more commonly utilized diameter, d, is used for the graphs, and the amplitudes have been adjusted such that the integral over the complete distribution is equal to one). The distribution shows two distinct peaks with maximums at 133 nm and 352 nm denoted as peak 1 and peak 2, which indicate the existence of two classes of particles. About 75% of the total intensity is scattered by the larger particles, and 25% by the smaller ones. The results obtained from the fractionated samples with the cumulant method are summarized in Table 2 and illustrated in Fig. 1 by arrows rising from the x-axis, the lengths of which are proportional to the mean intensity scattered by the different samples at the same incident intensity of the laser light source. The samples obtained after sucrose density gradient centrifugation were also too dilute for the determination of their chemical composition, and therefore were only characterized by their mean size.

When comparing results from cumulant analysis with results from CONTIN analysis with the $I(R)$ option, one has to remember that the mean size derived from $s(\Gamma)$ is numerically different from that derived from $I(R)$. Only in the limit with particles of a single size do the values of the two mean sizes become identical. The difference in the case of a size distribution is illustrated by the results obtained from the DG0 data with the two options of CONTIN and with the cumulant method. The mean diameter M_1/M_0 of $I(R)$ was 297 nm. The definition M_0/M_{-1} of $I(R)$ (Flamberg and Pecora 1984), on the other hand, yielded a mean diameter of 238 nm, and the same result was obtained from the analysis with the $s(\Gamma)$ option and using Eq. (3). Virtually the same mean diameter (239 nm) was obtained with the cumulant method with a four-cumulants fit. A three-cumulants fit was associated with a larger sum of squared residuals by nearly 30%, the residuals showed systematic deviations, and a larger mean size of 242 nm was obtained. The mean diameter derived from the mean linewidth was thus nearly 60 nm smaller than that obtained from the analysis with the $I(R)$ option. The two sizes, denoted as d_Γ and d_I, are indicated by arrows at the top line of the frame of Fig. 1. This difference for mathematical reasons probably explains the apparent left shift of the results from the unfractionated samples in Fig. 1, which is also supported by the finding that a corresponding plot of the cumulant results and the intensity distribution in terms of the linewidth does not show a systematic shift. Since the separation in terms of particle sizes is not expected to be complete in the fractionated samples, a change in the relative amounts of particles of different size would also result in a change of the mean size, and this change would be less for the mean size weighted by $I(R)$ than for the mean size weighted by $s(\Gamma)$. Accordingly, fractions DG1, DG2, and DG3 are expected to contain essentially particles from the group of large particles represented by the second peak, while DG5 will contain predominantly particles of sizes described by the first peak, and DG4 probably contains similar amounts of particles from both peaks. This assignment, however, can only be a tentative one at this stage, in particular since

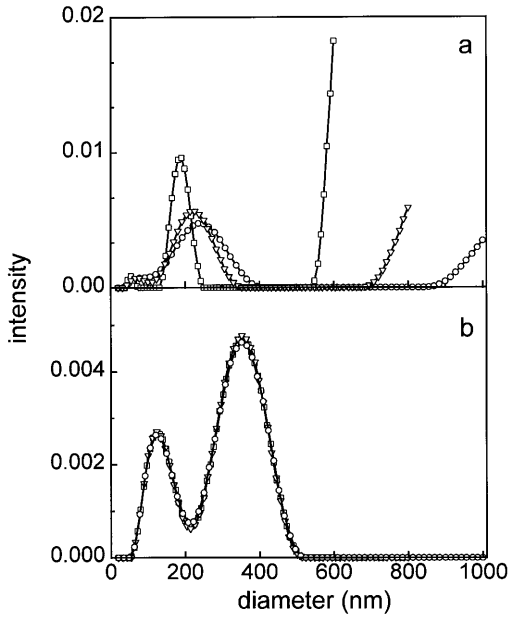

Fig. 2a, b Chylomicron sample DG0. Size distributions obtained from CONTIN analysis (PROB1 (α) ~ 0.5) with different size grids of 20–600 nm (□), 20–800 nm (▽), and 20–1000 nm (○) from original data (**a**) and from corrected data (**b**)

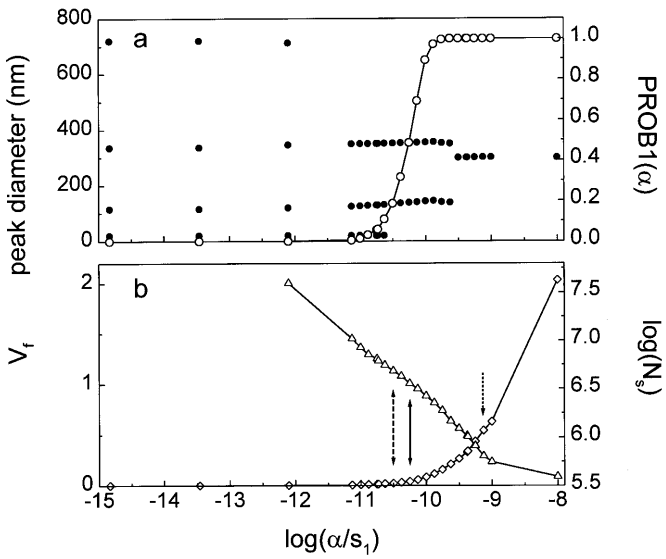

Fig. 3a, b Chylomicron sample DG0. Results of the complete CONTIN analysis of the corrected data using a size range of 20–720 nm. **a** Mean diameters of the various peaks of the size distributions (●) of the solutions obtained with different degrees of regularization and corresponding PROB1 (α) values (○). The four peaks at $\log(\alpha/s_1) \sim -15$ denote the characteristics of the size distribution of the least square or reference solution. **b** Relative change in variance V_f (◇) (Eq. 7) and logarithm of the solution norm N_s (△) (Eq. 8) of these solutions. The size distributions of the solutions of the confidence interval of the F-test are bimodal. The solutions selected by F-test [PROB1 (α) = 0.5] and stability plot are indicated by *solid* and *dashed arrows*. Owing to the noise content of these data the solution obtained from the F-test is slightly more strongly regularized than that from the stability plot, which also does not show a well-defined plateau region. The solution associated with a monomodal size distribution illustrated in Fig. 4 is marked by a *dotted arrow*

the mean diameters, d_Γ, of the fractionated samples are less accurate than that of the DG0 sample.

The bimodal size distribution obtained here (Fig. 1) has a peak size ratio of about 2.6 : 1. To show that two peaks with such a size ratio can be resolved from data with baselines larger than 10^8, we present details of our analysis and results obtained with computer-generated data. If the baseline were only of the order of 10^7, two peaks of a size ratio of 3 : 1 cannot be resolved, as demonstrated by Nyeo and Chu (1989) and Madani and Kaler (1991). Analysis of the original DG0 data without fitting an additional function yielded distributions with a peak ending with finite amplitude at the upper size limit, and which moved with this size limit if it was changed (Fig. 2a). Such side peaks, moving with the upper size limit, were found to be typical of relative baseline errors with a negative sign, and consistently the error was found to be $\Delta B/B = -7\times10^{-3}$. After correction of the data for normalization errors, a stable solution was obtained (Fig. 2b). The results of the complete CONTIN analysis are depicted in Fig. 3, where the mean peak diameters of the size distributions of each solution, the corresponding PROB1 (α) values, the logarithm of the solution norm, and the fractional increase in variance are plotted versus the regularization strength. The size distribution of the reference solution at $\alpha_0/s_1 = 1.5\times10^{-15}$ and the next two solutions up to $\alpha/s_1 \sim 10^{-12}$ exhibit four peaks, two of which are side peaks at the upper and the lower size limit, respectively. The increase in regularization strength is accompanied by a broadening of the peaks (not shown), and a simplification of the size distribution in terms of the number of peaks. In the confidence interval of the F-test the size distribution is bimodal, and the stability plot shows a region with minimum slope and a point of inflection. The solution of the inflection point [PROB1 (α) = 0.2] is less strongly regularized ($\alpha/s_1 = 3.2\times10^{-11}$) than the one selected by the F-test with PROB1 (α) = 0.5 ($\alpha/s_1 = 5.6\times10^{-11}$), but it is also a solution with a bimodal size distribution, and fits the data slightly better. The relative changes in variance of the two solutions are 2% and 4%, respectively (Fig. 3b). The statistical accuracy of the DG0 data was not very high, which is expressed in a fairly high variability of the size distributions with increasing regularization strength (Fig. 4a) and in the relatively large slope of the stability plot in the region of interest. The size distributions shown in Fig. 4a were from the confidence interval of the F-test and from above. The picture indicates the broadening of the peaks with increasing regularization strength, and at $\alpha/s_1 = 7.5\times10^{-10}$ (dotted arrow in Fig. 3b) the two peaks fused into one. This monomodal size distribution had nearly the same overall mean size and width as the bimodal size distributions selected by the F-test. A comparison of the differences of the two autocorrelation functions associated with these two size distributions with the noise in this data (Fig. 4b) provided strong evidence that the bimodal size distribution could be resolved from this data. The deviations of individual residual points from the difference curve are of the same order as the deviations from the zero line (which represents the solution with the bimodal size distribution in this difference plot), but the

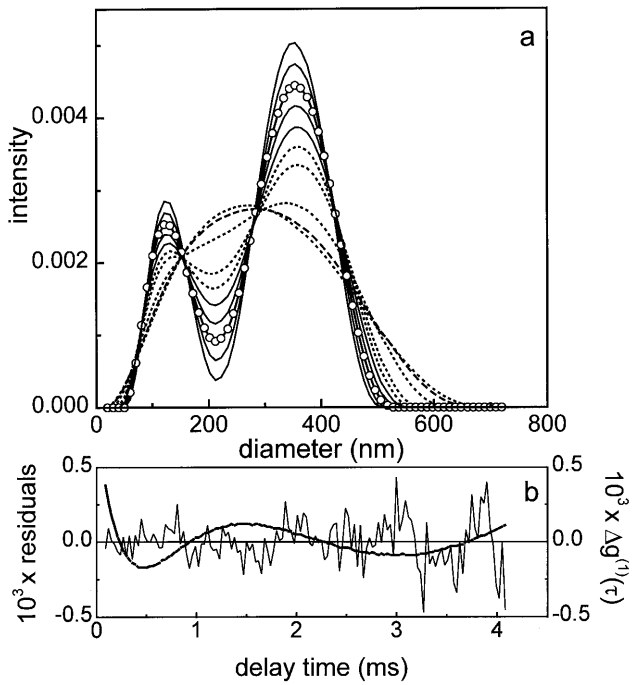

Fig. 4a, b Chylomicron sample DG0. **a** Size distributions from the confidence interval of the F-test (*solid lines*) and some of the size distributions obtained at stronger regularization strength (*dotted lines*). The size distribution selected by the F-test is marked (○), and the first monomodal size distribution with about the same overall mean size and width is characterized by a *broken line*. In **b** the differences of the electric field autocorrelation functions of these two solutions, $\Delta g^{(1)} = g^{(1)}_{\text{monomod}} - g^{(1)}_{\text{bimod}}$, are shown as a *dotted line*, together with the residuals of the "chosen" solution. Qualitatively, these two curves are similar, but quantitatively, the sum of squared differences to the difference curve is about 50% larger than the corresponding sum of the differences to the "chosen" solution

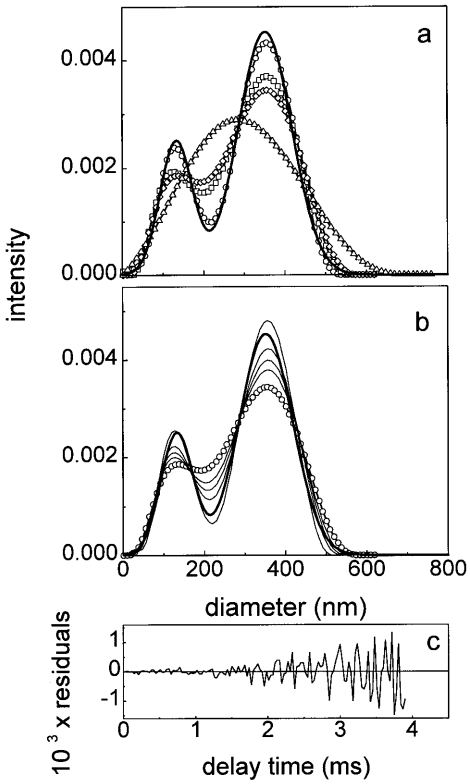

Fig. 5a–c Computer-generated data simulating the autocorrelation function of light scattered by a size distribution of two Gaussians (thick lines in **a** and **b**. **a** Results of CONTIN analysis from data containing different levels of noise: "exact" data (○), $B = 3\times10^9$ (□), $B = 2\times10^8$ (◇), $B = 1\times10^7$ (△). Solutions selected with PROB1 (α) ~0.5 resolve the bimodal character in all cases but one ($B = 1\times10^7$). Increase of the noise content broadens the distribution and shifts the regularization strength of the "chosen" solution to larger values: $\alpha/s_1 = 1.9\times10^{-13}$, 1.8×10^{-10}, 3.6×10^{-10}, and 1.3×10^{-8}. **b** For comparison with the experimental results displayed in Fig. 4a, some of the size distributions of the confidence interval of the F-test from the analysis of the data with $B = 2\times10^{-8}$ are shown. The size distribution of the "chosen" solution is indicated by (○), and the residuals of the field autocorrelation function of this solution are shown in **c**. The size distribution which overshoots the original size distribution is outside the confidence interval [Prob1 (α) = 0.04]

sums of squared deviations are different by more than 50%. In the case of the other chylomicron sample described below, data were of much higher statistical accuracy. Accordingly, the residuals were much smaller than the differences in the corresponding autocorrelation functions, and a very clear decision in favor of the solution with a bimodal size distribution could be made.

More strong evidence for being able to resolve two such peaks came from the results obtained with computer-generated data, which are shown in Fig. 5. We have analyzed four data sets of different noise content: the exact data with rounded seventh digit and three sets with noise corresponding to baseline values of 3×10^9, 2×10^8, and 1×10^7. The size distributions of the solutions determined with the F-test are displayed in Fig. 5a. In all cases but one a solution with a bimodal size distribution was recovered. Only the data with the highest noise content ($B = 1\times10^7$) gave a monomodal distribution, in agreement with the findings of Nyeo and Chu (1989). As expected, the CONTIN results approach the original size distribution best when the noise content was lowest. In the case of the practically noise-free data, the algorithm recovered this size distribution almost exactly, which was also found by Glatter et al. (1991) for a similar distribution.

The results from these analyses also indicate a property of the F-test, which explains why a monomodal distribution was produced from the data with the highest noise content, and the bimodal characteristic of this distribution could not be resolved. The appropriate degree of regularization is determined mainly from a given value of the relative change in variance. With increasing noise content the absolute change in variance increases, as does the regularization strength from which the "chosen" solution is taken. An increasing degree of regularization, however, implies increasing simplification of the size distribution. In the case of the data with $B = 10^7$ the shift on the regularization scale was so large that the region where the size distribution became monomodal was reached. At a considerably lower regularization strength the size distribution was still bimodal, but this solution was rejected by the test (see also Fig. 4 in Madani and Kaler 1991). Fitting an additional pa-

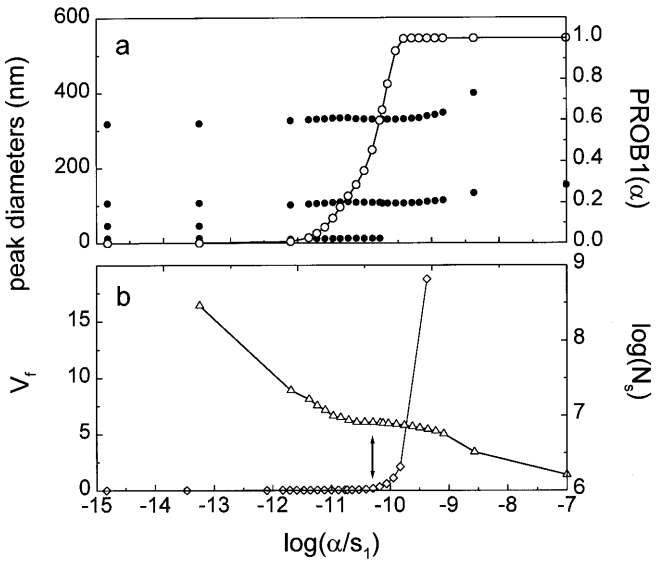

Fig. 6a, b Chylomicron II. Results of the complete CONTIN analysis of the corrected data ($\Delta B/B = -2.8\times10^{-3}$) using a size range of 20–600 nm. **a** Mean diameters of the various peaks of the size distributions (●) of the solutions obtained with different degrees of regularization and corresponding PROB1(α) values (○). **b** Relative change in variance V_f (◇) (Eq. 7) and logarithm of the solution norm N_s (△) (Eq. 8) of these solutions. The size distributions of the solutions of the confidence interval of the F-test are actually bimodal ones. The apparent peak with a small size is a side peak. The same solution is selected by the F-test and stability plot (*solid arrow*) from this statistically very accurate data, and correspondingly the stability plot exhibits a well-defined plateau

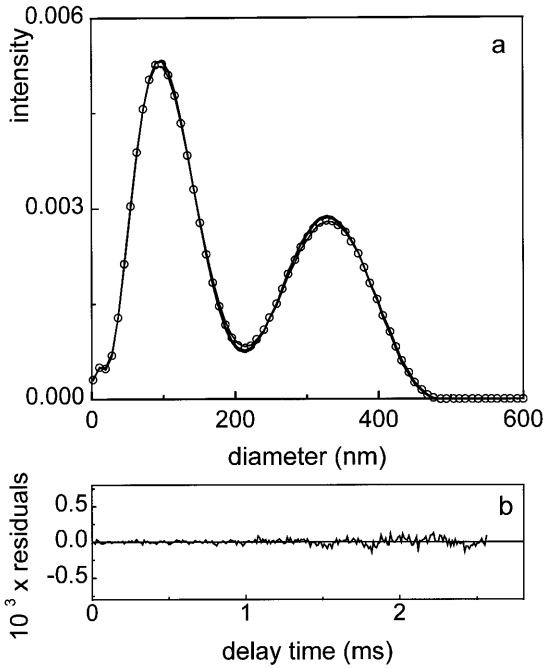

Fig. 7a, b Chylomicron II. **a** Size distributions from the confidence interval of the F-test. The size distribution selected by the F-test and stability plot is marked (○). In agreement with the high statistical accuracy of this data, there is practically no variation in the size distribution. **b** Residuals of the field autocorrelation function of this solution, which are more than one order of magnitude smaller than those depicted in Fig. 4b

rameter such as a constant background ("dust term") or a relative baseline error with NEF generally caused shifts on the regularization scale to stronger regularized solutions. Then, occasionally, a size distribution was simplified in their modality. This is one reason why we correct the data for normalization errors prior to final analysis, which is carried out without NEF.

To show the strong similarity of the results of simulated ($B=2\times10^8$) and experimental data (Fig. 4a), a series of size distributions are displayed in Fig. 5b. In both cases the peaks become progressively narrower with decreasing regularization strength, and in the case of the computer-generated data (Fig. 5b) approach the peaks of the theoretical size distribution. There is a size distribution which overshoots the original size distribution, but the corresponding solution was outside the lower limit of the confidence interval of the F-test. Such an overshoot was only observed when the noise content was relatively high. This finding supports the usefulness of Provencher's lower regularization limit of the confidence interval of the F-test. The residuals of the "chosen" solution of this analysis are displayed in Fig. 5c.

The statistical accuracy of the data from measurements on another chylomicron sample (chylomicron II) was much higher. This sample came from the same patient, but was taken on a different day, and the preparation included an additional centrifugation step. In addition, this sample was measured with a different detection system, based on a single mode fiber. We performed a series of 900 measurements on three different days. The temporal stability of the sample was checked (Ruf and Gould 1997). The data analyzed here were constructed from all 900 measurements. The error in the experimental baseline was determined as described above and the corrected data were analyzed without fitting for an additional function. Results from the complete analysis are shown in Fig. 6. The F-test and stability plot both selected the same solution ($V_f=0.03$), and the stability plot shows a region with a flat portion. Accordingly, the size distributions of this region (Fig. 7) does not show much variation. Also, owing to the higher statistical accuracy of the data, the solution selected by the two methods is from a smaller regularization strength ($\alpha/s_1 = 1.3\times10^{-11}$), and this is consistent with the results from the simulated data. The difference curve of the autocorrelation functions associated with this bimodal size distribution and a corresponding monomodal one is similar to that displayed in Fig. 4b with respect to the order of magnitude. The residuals depicted in Fig. 7b, however, are smaller by more than one order of magnitude, and thus a very clear decision can be made in favor of a solution with a bimodal size distribution. The finite amplitude of the distribution at the lower size limit is probably due to limitations of the detection system (i.e., afterpulsing). Mean peak sizes (108 nm and 330 nm) were somewhat smaller than for DG0 and the fraction of the light scattered by the peak of smaller sized particles was larger in this sample.

Discussion

The results from the analyses of the experimental and simulated chylomicron data show that two peaks with a size ratio of 2.6 : 1 can be resolved if measurements are made for a long enough time, in agreement with the results of other investigators (Bott 1983; Flamberg and Pecora 1984; Morrison et al. 1985; Hallett et al. 1991; Ruf et al. 1993). Morrison et al. (1985) used a very long measurement time (36 h) and were able to determine not only the mean peak sizes but also the widths of the two peaks of a binary mixture of latex standards of a size ratio of about 3 : 1 with excellent accuracy (the baseline of their combined data was between 3.1×10^{-9} and 1.2×10^{-10}, assuming that the mean scattered intensity was somewhere between 40 and 80 kcps). In the case of the DG0 data the size distributions of the solutions were more variable than in the case of the chylomicron II data because of the higher noise content. This difference in variability is also expressed in the two stability plots, which only showed a well defined plateau in the second case. Finally, the regularization strength at which both the F-test and stability plot selected their solutions was smaller in the case of the more accurate chylomicron II data, which is consistent with the results obtained with the simulated data.

The ability to resolve two peaks by the comparison of differences in autocorrelation functions with the residuals employed here is a method that can generally be applied to establish what can be resolved in given cases. In Ruf et al. (1993) this approach was used to show that a bimodal distribution with a peak size ratio of 1.5 : 1 cannot be distinguished from a monomodal size distribution of the same overall mean size and width from experimental data with a baseline of $B=3.75\times10^{8}$. The difference between the two autocorrelation functions was only of the order of 10^{-5} and was nearly one order of magnitude smaller than the noise. Analysis of computer-generated data with different noise contents is another way of establishing what can be resolved.

In the case of the low-noise chylomicron II data the two secondary selection methods, the F-test and the stability plot, yielded the same solution, while in the case of the chylomicron data DG0 the F-test with the PROB1 (α) ~ 0.5 criterion provided a slightly more strongly regularized or more damped solution. From analyses of other experimental data we know that the F-test with this probability value selects solutions which are frequently too strongly regularized, and this was the case with the computer-generated data with a higher noise content. This indicated that the commonly used PROB1 (α) ~ 0.5 selection criterion should be modified when data are of lower statistical accuracy so that the weakest regularized solution from the confidence interval of the F-test, which has the same complexity in terms of peak numbers, should be selected as the "chosen" solution. Alternatively, the stability plot can be used. However, since inflection points are not always unequivocally expressed on the stability plot, we recommend that both methods are used. When data accuracy is high enough this modification is not of importance as the size distribution is practically constant in the complete confidence interval of the test, as was found with data from liposomes (Ruf 1993).

The DLS measurements on the two chylomicron samples provided similar bimodal size distributions with about the same size range. The finding of a larger fraction of the smaller particles in the second sample is very likely due to the different dietary state of the patient. The bimodal size distribution is in good agreement with results from other investigations (Bierman et al. 1966; Fraser et al. 1968; Spooner et al. 1988). In the case of Spooner et al. (1988), a sample of rat lymph chylomicrons was fractionated by density gradient centrifugation, and their sizes were determined by gel chromatography (Sephacryl S-1000) and electron microscopy. Only the fraction of small-sized chylomicrons was analyzed by these two techniques, which consistently yielded mean diameters of 108 ± 7 nm and 111 ± 9 nm, respectively. As with our sample, the unfractionated rat lymph chylomicron sample contained a substantial fraction (in terms of mass) of larger particles ($d>250$ nm). In the elution profile of the chromatogram these appeared as a peak close to the void volume of the column and thus could not be characterized in terms of size. These large particles contained most of the triglycerides (only about 20% were recovered in the small particle fraction). When comparing DLS results with results from electron microscopy, one has to obtain the corresponding number distribution. This can be derived in principle by using the light scattering properties of the particles, as has been done, for example, for unilamellar liposomes (Hallett et al. 1989; Kojro et al. 1989; Hallett et al. 1991; Schurtenberger and Newman 1993; Egelhaaf et al. 1996). To obtain a reasonable estimate, the intensity distribution must be known with high accuracy and proper conversion factors are needed (a detailed discussion on this topic can be found in the article of Bott 1987). We think that our intensity distributions meet this requirement to a certain extent, but lipoproteins require more complicated conversion factors than liposomes. The constituents of lipoprotein particles, triglycerides, cholesterol, lipids, and a few protein molecules are not homogeneously distributed within the particle. A proper conversion factor must take into account this anisotropic distribution of the scattering elements with their different refractive indices. However, since chylomicrons with a diameter of about 100 nm have a protein content of only about 2% (w/w) and most of the hydrocarbons are triglycerides (84% w/w), we have employed the scattering amplitude functions for isotropic spherical particles of Mie as conversion factors (Bott 1987) to obtain a first estimate of the number distribution.

This estimation indicated that the overwhelming majority the of particles were small ones (probably in excess of 95%) with sizes between 40 nm and 200 nm. Moreover, peak 1 of this number distribution had a maximum below 100 nm, which suggested that this peak involved not only chylomicrons.We know that this particular human thoracic duct lymph contains apolipoprotein (apo) B-100 (42.9 μg/ml), which is normally associated with hepatocyte derived particles such as VLDL, IDL, and LDL, and

19.1 μg/ml of apo B-48 (Lovegrove et al. 1996), which is only associated with enterocyte-derived chylomicrons in humans. Chylomicrons are quoted as having a size range from 80–500 nm (Mills et al. 1984). These particles contain apo B-48, but there is currently a dispute as to whether the enterocyte can produce up to 10% of particles containing apo B-100 in place of apo B-48 (Hoeg et al. 1990; Levy et al. 1990). However, since lipoprotein particles are expected to contain only one molecule of apo B per particle, and allowing for the fact that the molecular size of apo B-48 is approximately half that of apo B-100, the bimodal distribution is not explained by there being two types of particle – one associated with apo B-48 and the other with apo B-100. The protein ratio indicates that the two types of apoprotein-carrying particles are present in similar numbers, and the estimated number distribution indicated that the majority of the particles are smaller ones. This suggests that peak 1 represents a mixture of small chylomicrons derived from those enterocytes which were not receiving a supply of triglyceride, and apo B-100 containing particles. The latter are very likely VLDLs having a size range of 30–80 nm. Such a mixture is consistent with the finding of a mean diameter of peak 1 of the estimated number distribution well below 100 nm, that is, below the size which is considered as typical of chylomicrons. The few percent of larger particles in terms of numbers of peak 2 are probably dietary triglyceride-rich chylomicrons. It is worth noting that the difference in triglyceride loading of the two sizes of particles is about 64-fold. The finding of apolipoprotein (apo) B-100 carrying lipoproteins, which are smaller than chylomicrons, in the mixture forming peak 1, however, also shows that our assumption of isotropic spheres was too simple. To obtain an improved estimate of the number distribution of peak 1, one has to use conversion factors that take the internal structure of the particles and the varying protein content into account, which in the case of VLDLs changes with decreasing size from about 4% to 11%.

The results from these studies showed that the intensity-weighted size distribution, the estimate of the number distribution together with the contents of the specific proteins associated with different types of lipoprotein particles, has already yielded a fairly detailed description of these samples. This indicates that measurements on similarly prepared samples can be employed directly for studies, for example, of processes involved in unloading of these triglyceride-rich lipoproteins by the action of lipases. A much more detailed characterization of lipoprotein particles, however, would be achieved if the components of such samples were separated, e.g. by density gradient centrifugation, prior to size determinations by DLS.

Acknowledgements The authors wish to thank Dr. S. W. Provencher for providing CONTIN and valuable discussions, Dr. R. Finsy for providing the subroutine for calculations of Mie scattering amplitude functions, Dr. A. Topp for extending our CONTIN version to 70 grid points, and Dr. E. Grell for valuable discussions. This work was partially supported by the Deutsche Akademische Austauschdienst (ARC), the BBSRC, and the British Council.

References

Biermann EL, Hayes TL, Hawkins JN, Ewing AM, Lindgreen FT (1966) Particle-size distribution of very low density plasma lipoproteins during fat absorption in man. J Lipid Res 7:65–72

Bott SE (1983) Polydispersity analysis of QELS data by a smooth inverse Laplace transform. In: Dahneke BE (ed) Measurement of suspended particles by quasi-elastic light scattering. Wiley, New York, pp 129–157

Bott SE (1987) Submicron particle sizing by photon correlation spectroscopy: use of multiple-angle detection. In: Provder T (ed) Particle size distribution. (ACS symposium series, vol 223) American Chemical Society, Washington, pp 74–88

Chu B, Ford JR, Dhadwal HS (1985) Correlation function profile analysis of polydisperse macromolecular solutions and colloidal suspensions. In: Hirs CHW, Timasheff SN (eds) Methods in enzymology, vol 117. Academic Press, San Diego, pp 256–297

Edelstein C, Scanu AM (1986) Precautionary measures for collecting blood destined for lipoprotein isolation. Methods in enzymology, vol 128. Academic Press, San Diego, pp 151–155

Egelhaaf SU, Wehrli E, Müller M, Adrian M, Schurtenberger P (1996) Determination of the size distributions of lecithin liposomes; a comparative study using freeze fracture, cryoelectron microscopy and dynamic light scattering. J Microsc 184:214–228

Flamberg A, Pecora R (1984) Dynamic light scattering study of micelles in a high ionic solution. J Phys Chem 88:3026–3033

Fraser R, Cliff WJ, Courtice FC (1968) The effect of dietary fat load on the size and composition of chylomicrons in thoracic duct lymph. Q J Exp Physiol 53:390–398

Georgalis Y, Ruf H, Grell E (1987) Photon correlation spectroscopy of membrane model systems. In: Burgen ASV, Roberts GCK, Aner BM (eds) Topics in molecular pharmacology, vol 4. Elsevier, Amsterdam, pp 1–20

Gisler T, Ruger H, Egelhaaf SU, Tschumi J, Schurtenberger P, Ricka J (1995) Mode selective dynamic light scattering – theory versus experimental realization. Appl Opt 34:3546–3553

Glatter O, Sieberer J, Schnablegger H (1991) A comparative study on different scattering techniques and data evaluation methods for sizing of colloidal systems using light scattering. Part Part Syst Charact 8:274–281

Grundy SM, Mok HYI (1965) Chylomicron clearance in normal and hyperlipidaemic man. Metabolism 25:1225–1291

Hallett FR, Craig T, Marsh J, Nickel B (1989) Particle size analysis: number distributions by dynamic light scattering. Can J Spectrosc 34:63–70

Hallett FR, Watton J, Krygsman P (1991) Vesicle sizing: number distributions by dynamic light scattering. Biophys J 59:357–362

Hoeg JH, Sviridov DD, Tennyson GE, Demonsky SJ, Meng MS, Bojanovski D, Safonova IG, Repin VS, Kuberger MB, Smirnov VN, Higuchi K, Gregg RE, Brewer HB (1990) Both apolipoproteins B-48 and B-100 are synthesized and secreted by human intestine. J Lipid Res 31:1761–1769

Karpe F, Hamsten A (1994) Determination of apolipoprotein B_{48} and B_{100} in triglyceride-rich lipoproteins by analytical SDS-page. J Lipid Res 35:1311–1317

Kojro Z, Lin SQ, Grell E, Ruf H (1989) Determination of internal volume and volume distribution of lipid vesicles from dynamic light scattering data. Biochim Biophys Acta 985:1–8

Koppel DE (1972) Analysis of macromolecular polydispersity in intensity correlation spectroscopy: the method of cumulants. J Chem Phys 57:4814–4820

Levy E, Rochette C, Londono I, Roy CC, Milne RW, Marcel YL, Bendayan M (1990) Apolipoprotein B-100: immunolocalization and synthesis in human intestinal mucosa. J Lipid Res 31:1937–1947

Lide DR (ed) (1975–1976) Handbook of chemistry and physics, 56th ed. CRC Press, Cleveland

Lindgren FT, Jensen LC, Hatch FT (1972) The isolation and quantitative analysis of serum lipoproteins. In: Nelson GJ (ed) Blood lipids and lipoproteins: quantitation, composition, and metabolism. Wiley, New York, pp 181–274

Lovegrove JA, Isherwood SG, Jackson KG, Williams CM, Gould BJ (1996) Quantitation of apolipoprotein B-48 in triacylglycerol-rich lipoproteins by a specific enzyme-linked immunosorbent assay. Biochim Biophys Acta 1301: 221–229

Madani H, Kaler EW (1991) Measurement of polydisperse colloidal suspensions with quasielastic light scattering. Part Part Syst Charact 8: 259–266

Mills GA, Lane PA, Weech PK (1984) The isolation and purification of plasma lipoproteins. In: Burdon RH, Van Knippenberg PH (eds) A guidebook to lipoprotein technique. (Laboratory techniques in biochemistry and molecular biology) Elsevier, Oxford, pp 18–116

Morrison ID, Grabowski EF, Herb CA (1985) Improved techniques for particle size determination by quasielastic light scattering. Langmuir 1: 496–501

Nenseter MS, Rustan AC, Lund-Katz S, Soyland E, Maelandsmo G, Phillips MC, Drevon CA (1992) Effect of dietary supplementation with n-3 polyunsaturated fatty acids on physical properties and metabolism of low density lipoprotein in humans. Arterioscler Thromb Vasc Biol 12: 369–379

Nyeo SL, Chu B (1989) Maximum-entropy analysis of photon correlation spectroscopy data. Macromolecules 22: 3998–4009

Phillips DL (1962) A technique for the numerical solution of certain integral equations of the first kind. J Ass Comut Mach 9: 84–97

Pike ER, Watson D, McNeil Watson F (1983) Analysis of polydisperse scattering data II. In: Dahneke BE (ed) Measurement of suspended particles by quasi-elastic light scattering. Wiley, New York, pp 107–128

Provencher SW (1979) Inverse problems in polymer characterization: direct analysis of polydispersity with photon correlation spectroscopy. Makromol Chem 180: 201–209

Provencher SW (1982a) A constrained regularization method for inverting data represented by linear algebraic or integral equations. Comput Phys Commun 27: 213–227

Provencher SW (1982b) CONTIN: a general purpose constrained regularization program for inverting noisy linear algebraic and integral equations. Comput Phys Commun 27: 229–242

Provencher SW (1992) Low-bias macroscopic analysis of polydispersity. In: Harding SE, Sattelle DB, Bloomfield VA (eds) Laser light scattering in biochemistry. Royal Society of Chemistry, Cambridge, pp 92–111

Provencher SW, Hendrix J, De Maeyer L, Paulussen N (1978) Direct determination of molecular weight distributions of polystyrene in cyclohexane with photon correlation spectroscopy. J Chem Phys 69: 4273–4276

Ruf H (1989) Effects of normalization errors on size distributions obtained from dynamic light scattering data. Biophys J 56: 67–78

Ruf H (1993) Data accuracy and resolution in particle sizing by dynamic light scattering. Adv Colloid Interface Sci 46: 333–342

Ruf H, Gould BJ (1997) The use of dynamic light scattering for the determination of size distributions of chylomicrons from human lymph. In: Priezzhev A, Asakura T, Leif RC (eds) Optical diagnostic of biological fluids and advanced techniques in analytical cytology, vol 2982. SPIE – The International Society for Optical Engineering, San Jose, Calif, pp 206–213

Ruf H, Grell E, Stelzer EHK (1992) Size distribution of submicron particles by dynamic light scattering measurements: analyses considering normalization errors. Eur Biophys J 21: 21–28

Ruf H, Haase W, Wang WQ, Grell E, Gärtner P, Michel H, Dufour JP (1993) Determination of size distributions of submicron particles by dynamic light scattering experiments taking into account normalization errors. Prog Colloid Polym Sci 93: 159–166

Saleh B, Cardoso MF (1973) The effect of channel correlation on the accuracy of photon counting digital autocorrelation. J Phys A 6: 1897–1909

Schnablegger H, Glatter O (1991) Optical sizing of small colloidal particles: an optimized regularization technique. Appl Opt 30: 4889–4896

Schurtenberger P, Newman ME (1993) Characterization of biological and environmental particles using static and dynamic light scattering. In: Buffle J, van Leeuwen HP (eds) Environmental particles, vol 2. Lewis, Boca Raton, pp 37–115

Siegert AJF (1943) MIT Rad Lab Rep No 465

Spooner PJR, Bennett Clark S, Gantz DL, Hamilton JA, Small DM (1988) The ionization and distribution behavior of oleic acid in chylomicrons and chylomicron-like emulsion particles and the influence of serum albumin. J Biol Chem 263: 1444–1453

Stelzer EHK, Ruf H, Grell E (1983) Analysis and resolution of polydisperse systems. In: Schulz-DuBois EO (ed) Photon correlation techniques in fluid mechanics, vol 38. Springer, Berlin Heidelberg New York, pp 329–334

Vuaridel-Bonanomi ES, Weder HG (1991) The use of liposomes for the preparation of protein-free lipid emulsions models of chylomicron remnants. J Microencaps 8: 203–214

Zilversmit BD (1969) Chylomicrons. In: Tria E, Scanu AM (eds) Structural and fundamental aspects of lipoproteins in living systems. Academic Press, London, pp 329–368